ACS APPLIED MATERIALS & INTERFACES

Research Article

www.acsami.org

Smac Therapeutic Peptide Nanoparticles Inducing Apoptosis of Cancer Cells for Combination Chemotherapy with Doxorubicin

Mingxing Li,[†] Peng Liu,[‡] Guanhui Gao,[‡] Jizhe Deng,[‡] Zhengyin Pan,[‡] Xu Wu,[†] Gaofeng Xie,[‡] Caixia Yue,[§] Chi Hin Cho,[†] Yifan Ma,[‡] and Lintao Cai*[,‡]

[‡]Guangdong Key Laboratory of Nanomedicine, CAS Key Laboratory of Health Informatics, Institute of Biomedicine and Biotechnology, Shenzhen Institutes of Advanced Technology, Chinese Academy of Sciences, Shenzhen 518055, China

[†]School of Biomedical Sciences, The Chinese University of Hong Kong, Hong Kong, SAR, China

[§]Institute of Nano Biomedicine and Engineering, Key Laboratory for Thin Film and Microfabrication Technology of the Ministry of Education, Shanghai Jiao Tong University, Shanghai 200240, China

Supporting Information

ABSTRACT: Smac-conjugated nanoparticle (Smac-NP) was designed to induce the apoptosis of cancer cells and as a drug carrier for combination therapy. It contained three parts, a SmacN7 peptide which could induce apoptosis of cancer cells by interacting with XIAPs, the cell penetrating domain rich in arginine, and four hydrophobic tails for self-assembled Smac-NP. We demonstrated that Smac-NPs exerted an antitumor effect in breast cancer cell MDA-MB-231 and nonsmall lung cancer (NSCLC) cell H460, which efficiently inhibited cancer cells proliferation without influencing normal liver cell lines LO2. Smac-NPs also significantly induced apoptosis of MDA-MB-231 and H460 cells through activating pro-caspase-3, down-regulating the expression of antiapoptotic protein Bcl-2 and up-regulating the pro-apoptotic protein Bax. Furthermore, Smac-NPs could be explored as a drug delivery system to load hydrophobic drug such as DOX for combination therapy. The DOX-loaded nanoparticles (DOX-Smac-NPs) exhibited higher cellular uptake efficiency and antitumor effect. Our work provided a new insight into therapeutic peptides integrated with drug simultaneously in one system for cancer combination treatment.

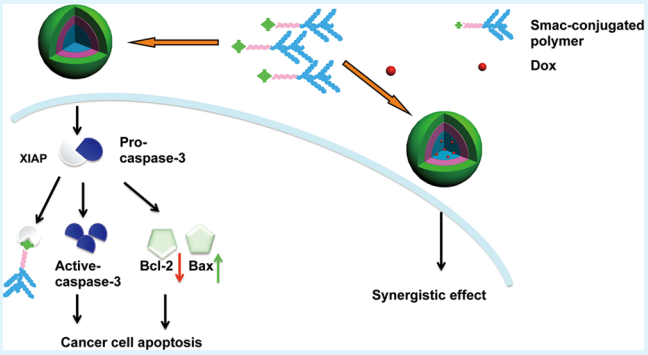

KEYWORDS: *Smac, therapeutic peptides, drug delivery, combination therapy*

INTRODUCTION

Inhibition of apoptosis plays an important role in human disease, especially in cancer, where apoptosis regulators become more attractive as molecular targets to treat cancer. The inhibitor of apoptosis proteins (IAP) was previously reported as involving in the suppression of cancer cell apoptosis by preventing the activation of pro-caspases.[1,2] However, second mitochondria-derived activator (Smac) is a recently identified protein released from mitochondria, which promotes caspase activity by binding to IAP, abolishing the inhibitory activity of IAP in apoptosis.[3−5]

Structural analysis has proved that N-terminal residues of Smac were essential for Smac function in interaction with BIR3 domain of IAP.[1,6−8] A short 7-residue peptide derived from the Smac N-terminus, which was named as SmacN7, was able to promote the activation of caspase-3, raising the possibility of using small peptides or peptide mimics to treat cancer cells. It has been reported that transfection of Smac gene into human leukemic cell could inhibit cell proliferation and induce cell apoptosis. Meanwhile, SmacN7 was also designed to conjugate a cell membrane permeable polyarginine peptide (R8). SmacN7R8 strongly induced apoptosis of human lung cancer cell H460.[9] Several studied also reported some Smac mimetics derived from Smac peptide to induce cancer cell apoptosis and also increase cell death combined with chemotherapy.[10−13] Sun et al. had explored new small molecule Smac mimetics, SM164, which could efficiently induce the apoptosis and radiosensitization of cancer cells.[10,14−18] Other Smac mimetics such as JP1201 also has been reported.[19] However, the application of therapeutic peptides needs to be improved because of its limitations. It is difficult to control the distribution of the peptides in vivo. It is also important to increase the cellular uptake of the peptide and to find a way that the peptides can directly target the tumor site to kill cancer cells. Thus, site-specific peptides and cell penetrating peptides were generated for treatment of cancers.[20−22]

Currently, biocompatible and versatile nanoparticles become widely used in tumor diagnosis[23−25] and targeted tumor

Received: January 12, 2015
Accepted: March 27, 2015
Published: March 27, 2015

DOI: 10.1021/acsami.5b00329
ACS Appl. Mater. Interfaces 2015, 7, 8005−8012

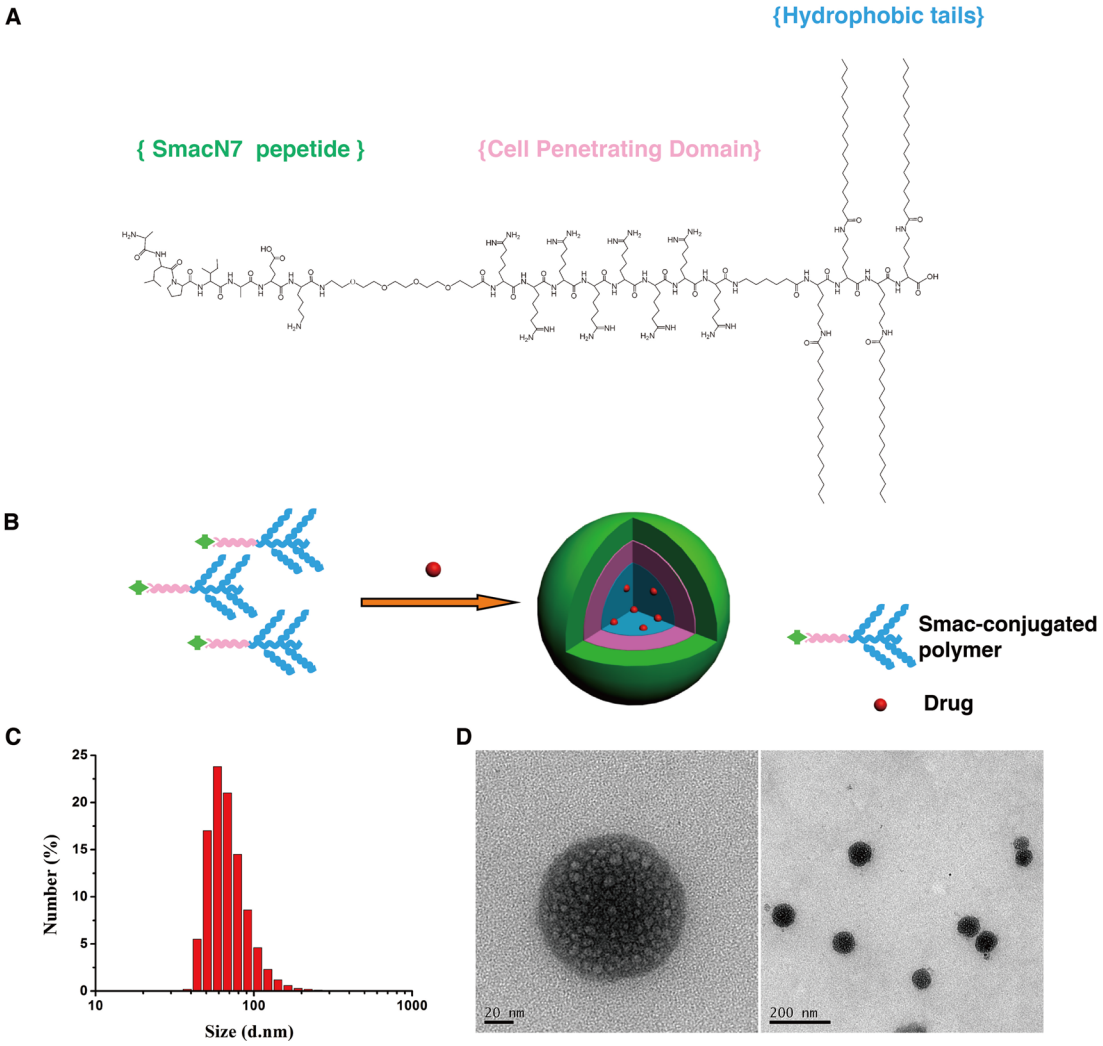

Figure 1. Characterization of Smac-nanoparticles. (A) Structure of Smac-NPs contains three main functional parts. Part I, SmacN7 peptide, which could induce apoptosis of cancer cells by interacting with XIAPs; Part II, cell penetrating domain rich in arginine; Part III, four hydrophobic tails, which could self-assemble in nanoparticles. (B) Schematic of illustration of self-assembled micelle and loading of drug. (C) Size analysis of Smac-NPs by DLS. (D) Transmission electronic microscopic image of Smac-NPs.

therapy, in which biodegradable nanoparticles are broadly designed to delivery hydrophobic chemotherapeutics with passively and actively targeted to tumor site effectively as well as cationic micelles for gene delivery.[26,27] A surfactant-like tetra-tail $[(C_{18})_2K]_2KR_8GRGDS$ amphiphilic peptide was designed for targeted drug delivery.[28] The polypeptide cationic nanoparticles have been developed for combination tumor therapy via mediating codelivery of doxcetaxel and Bcl-2 siRNA.[29] Meanwhile, DOX/ICG loaded lipid-polymer micelles could be used for effective chemo-photothermal synergistic therapy, which could also overcome the multidrug resistant of cancer cells.[30] Nanoparticles codelivery chemical therapeutics including DOX/paclitaxel and gene can overcome the drug resistant of cancer cells,[31−33] which also enhance the antitumor effect of chemotherapeutics and broaden the perspectives of developing new efficient nanoparticles.[32]

Herein, we developed a novel therapeutic Smac nanoparticle (Smac-NP) which contains site-specific peptide that can not only induce the apoptosis of cancer cells but also function as drug carriers. Smac-NPs were designed using SmacN7 peptide as the head, and cell penetrating peptide (CPP) in the middle, and also four hydrophobic aliphatic tails which were able to self-assemble into nanoscale micelles. These three parts enhance cellular uptake of nanoparticle. In more details, SmacN7 peptide was able to combine the XIAP to induce cell apoptosis by eliminating the antiapoptotic function of XIAP. Cell penetrating peptide, which was rich in arginine, performed enhanced cellular uptake of the Smac-NPs crossing through the cell membrane. The cytotoxicity, cellular uptake and its antitumor efficiency of Smac-NPs were investigated. The well-defined therapeutic Smac nanoparticles are confirmed to play the important role in the treatment with cancer, and its combination therapy with the chemotherapeutic drugs provides a new insight into therapeutic peptide nanoparticle-mediated drug delivery.

EXPERIMENTAL SECTION

1. Materials. Smac-conjugated polymer and SmacN7 were synthesized by Apeptide (Apeptide Co., Ltd., China). Doxorubicin hydrochloride (DOX·HCl) was purchased from Melonpharma (Dalian Meilun biology technology CO., Ltd., China). The human hepatic cell line LO2, breast cancer cell line MDA-MB-231, and hepatocellular carcinoma cell line H460 were purchased from American Type Culture Collection (ATCC). RIPM1640 and fetal bovine serum (FBS) were purchased from GIBCO (Life technologies, USA).

DOI: 10.1021/acsami.5b00329
ACS Appl. Mater. Interfaces 2015, 7, 8005−8012

2. Synthesis and Characterization of Smac-Nanoparticles. The Smac-conjugated nanoparticles was designed by our lab and synthesized by Apeptide. The average diameters and zeta potential of the micelles were determined by Laser Particle Size Analyzer (Malvern Instruments, Worcestershire, UK). The morphology of micelles was characterized by using Transmittance Electron Microscope (TEM) with accelerated voltage of 200 kV.

3. Preparation of DOX-Loaded Smac-NPs. DOX·HCl (1 mg) was added to $CHCl_3$ (1 mL) and solubilized by the addition of 3.0 equiv of triethylamine with stirring for 1 h. Smac-NP was dissolved in PBS to the concentration of 1 mg/mL. The $CHCl_3$ solution of DOX was added to the stirring Smac-NPs solution, forming the oil/water emulsion. The o/w emulation was kept stirring for 2−4 h at room temperature and then distilled at 37 °C under reduced pressure by vacuum steaming apparatus. Free DOX was removed from Smac-NPs micelles by ultrafiltration (Millipore, USA). Drug loading content of DOX-loaded in the Smac-NPs was determined by fluorescence at 480 nm with the maximum absorption at 590 nm (FLS920, Dinburgh Instruments). Drug loading efficiency (DLE) and drug loading content (DLC) of Smac-NPs were calculated by the following formulas

$$\mathrm{DLC}(\%) = W_{\text{loaded drug}}/W_{\text{drug-loaded nanoparticles}} \times 100\%$$

$$\mathrm{DLE}(\%) = W_{\text{loaded drug}}/W_{\text{free drug}} \times 100\%.$$

4. In Vitro Cellular Uptake Studied by Laser Confocal Microscopy. MDA-MB-231 and H460 cells, which were seeded in Lab-Tek 8-well chamber system (Nunc, Thermo Scientific) and incubated 24 h, were treated with FAM labeled SmacN7 and Smac-NPs for 1 h. Then, the cellular uptake of SmacN7 and Smac-NPs were detected by confocal laser scanning microscopy.

The confocal microscopy assay was also performed to detect the cellular uptake of free DOX and Dox-Smac-NPs (1 μg/mL of DOX concentration) in the following studies.

5. Cytotoxicity Assay. The effect of SmacN7, Smac-NPs and DOX-loaded Smac-NPs on cell proliferation was evaluated by the Cell Counting Assay Kit-8 (CCK-8, Dojindo Laboratory, Kumamoto, Japan). LO2, MDA-MB-231, and H460 cells (3×10^3 cells per well) were seeded in 96-well plates and incubated in RPMI1640 medium for 24 h. The medium was then replaced by medium within SmacN7 or Smac-NPs at various concentrations from 1 to 20 μM. Twenty-four hours later, 10 μL of CCK-8 solution was added to each well, and the cells were incubated for another 2 h. The absorbance values (A) were then measured at 450 nm using a microELISA reader (Synergy2, BioTek). Cell viability (%) was expressed by the following equation: Cell viability (%) = $(A_{\text{sample}} - A_{\text{blank}})/(A_{\text{control}} - A_{\text{blank}}) \times 100\%$.

The cytotoxicity assay was also performed in MDA-MB-231 and H460 cells in the presence of DOX-loaded Smac-NPs compared with free DOX at different concentration of DOX from 0.004 to 0.02 μg/mL.

6. Flow Cytometry Assay. *6.1. Cell Apoptosis Assay.* Cell apoptosis was analyzed by using Dead Cell Apoptosis Kit with Annexin V Alexa Fluor 488 & PI (Molecular Probes, Life technologies, USA). MDA-MB-231 and H460 cells were seeded in 24-well plate with 5×10^4 cells per well and were incubated. The cells were treated with Smac-NPs at the concentration of 7.5 μM and 10 μM for 8 and 24 h, respectively. The treated cells as well as control were collected and stained by Annexin V and PI (1 μg/mL) for 15 min at room temperature. The apoptosis rate was detected by Flow cytometer (BD).

6.2. Cell Uptake Assay. MDA-MB-231 and H460 cells, which were seeded in 24-well plate and incubated 24 h, were treated with free DOX and DOX-loaded Smac-NPs at the same concentration of DOX (0.01 μg/mL) for 1, 2, 4, and 8 h. The treated cells as well as control were then also collected and detected by the flow cytometer the same as before.

7. Western-Blot Assay to Evaluate the Activation of Pro-Caspase-3 and the Expression of Bcl-2. MDA-MB-231 and H460 cells were separately seeded in 12-well plates with a 1×10^5 concentration and incubated for 24 h at 37 °C. Then the cells were treated with Smac-NPs at the same concentration as used in cell apoptosis assays for 24 h. Treated cells were lysed in RIPA buffer containing a cocktail of protease inhibitors and phosphatase inhibitors. Equal amounts of protein sample (10 μg) was separated by 12% SDS-PAGE and transferred to PVDF membrane (Millipore, Bedford, MA, USA) using the Bio-Rad semidry transfer system. The following antibodies were used for Western-blot: anti-α-tubulin (Abcam, USA), antipro-caspase-3(Abcam, USA), anti-Bcl-2(Sigma, USA), anti-β-actin (Cell signaling Technology(CST), USA), anti-Bax (CST, USA), anti-NF-kB (CST, USA), and anti-Caspase-8 (CST, USA).

8. Statistical Analysis. All experiments were repeated at least three times. Student's t test statistical analysis was performed with Graphpad Prism 6.

RESULTS AND DISCUSSION

Synthesis and Characterization of Smac-Nanoparticles (Smac-NPs). Smac-conjugated polymer was designed and illustrated in Figure 1A. Smac-conjugated polymer contains three main parts, the SmacN7 peptide, which could combine to the XIAP to induce apoptosis; the cell penetrating domain rich in arginine; and the hydrophobic part, which contains four tails. High-performance liquid chromatography (HPLC) was used to measure the purity of Smac-NPs, and the chemical structure of Smac-conjugated polymer was confirmed by mass spectrum (MS) analysis (Supporting Information, Figures S1 and S2). The Smac-conjugated polymer could self-assemble into nanoparticles in aqueous solution. The size of Smac-NPs was determined to 80 nm in average by using dynamic light scattering (DLS) as shown in Figure 1C. The result of TEM (Figure 1D) demonstrated that the self-assembled micelles possessed a distinct smooth spherical structure with the size of 100 nm. The size of nanoparticles was evaluated for over 10 days and stability is shown in Figure S3 (see the Supporting Information).

Cellular Uptake of Smac-NPs by Confocal Microscopy. To investigate cellular uptake efficiency of Smac-NPs, we used SmacN7 as control. Figure 2 showed confocal microscopy imaging for the cellular uptake of SmacN7 and Smac-NPs in breast cancer cell MDA-MB-231 and lung cancer cells H460. MDA-MB-231 and H460 cells were treated with FAM labeled SmacN7 and Smac-NPs at the Smac concentration of 20 μM for 2 h. As shown in Figure 2, green fluorescence was neither observed in MDA-MB-231 cells nor in H460 cells after treatment with SmacN7. However, in contrast of the SmacN7, we detect stronger green fluorescence of Smac-NPs in MDA-MB-231 and H460 cells, where the distribution of Smac-NPs were detected in both cell membranes and cytoplasma, suggesting that Smac-NPs can not only insert in cell membranes but also translocate into cytoplasma. The cell penetrating peptide, which was rich in arginine of Smac-NPs, greatly improved the cellular uptake efficiency. Overall, Smac-NPs provided a good platform for Smac therapeutic peptide in the functional role of cell apoptosis and drug delivery.

Antiproliferation Effect of Smac-NPs on MDA-MB-231 and H460 Cells. To study the effect of Smac-NPs on the proliferation of both cancer cells and normal cells, CCK-8 assay was performed to examine the cytotoxicity of Smac-NPs and SmacN7 in MDA-MB-231, H460 as well as normal cell lines LO2. As shown in Figure 3, SmacN7 showed little cytotoxicity effect on all three kinds of cells, which might due to less intracellular uptake efficiency of SmacN7. However, Smac-NPs could significantly inhibit the proliferation of MDA-MB-231 and H460 when the concentration were increased more than 10 μM, suggesting that Smac-NPs could interact with cancer cells and inhibit breast cancer and liver cancer cell growth. However,

DOI: 10.1021/acsami.5b00329
ACS Appl. Mater. Interfaces 2015, 7, 8005−8012

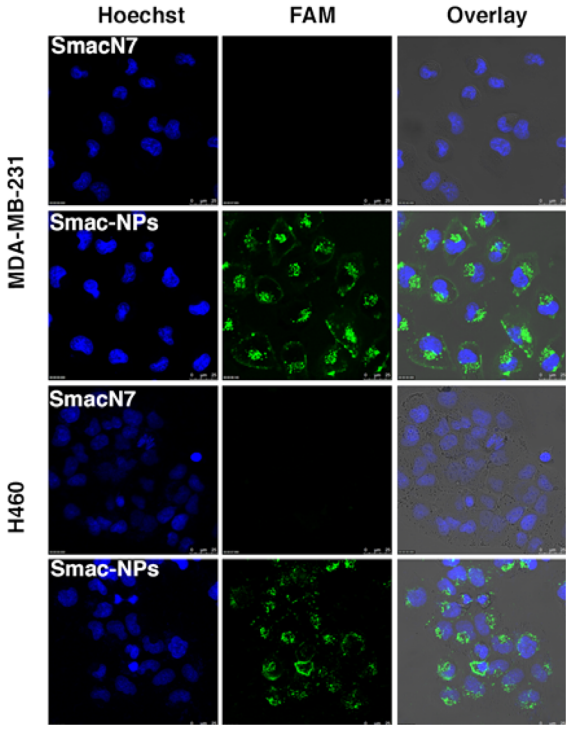

Figure 2. Confocal microscopy imaging for cellular uptake of SmacN7 and Smac-NPs in MDA-MB-231 and H460 after incubation for 2 h. The dose of SmacN7 and Smac-NPs were 10 μM. And SmacN7 and Smac-NPs were labeled with fluorescein amidite (FAM, green).

Smac-NPs had no cytotoxicity effect on normal cells LO2. Thus, Smac-NPs might function as a novel efficient therapeutic peptide drug to suppress cancer cells without influence on normal cells.

Inducing Cell Apoptosis by Smac-NPs. It has been reported that the endogenous peptide Smac could activate cell apoptosis pathways through interacting with XIAP and relieve its role in apoptosis inhibition.[3,34] To further investigate the function of Smac-NPs, we used flow cytometer assay to examine whether Smac-NPs could induce cell apoptosis. MDA-MB-231 and H460 cells respectively exposed to Smac-NPs at 5 μM and 10 μM for 8 and 24 h. Figure 4 revealed that Smac-NPs could induce apoptosis in both MDA-MB-231 and H460. Furthermore, Smac-NPs could induce cell apoptosis of MDA-MB-231 in a concentration-dependent manner. In details, the total apoptosis cells for 8 h increased significantly as concentration increased, from 10.4% at 5 μM to 67.1% at 10 μM. Moreover, cell number of late apoptosis stage was increased as time was going on from 8 to 24 h at concentrations of both 5 and 10 μM. Consistently, cell apoptosis of H460 was also induced by Smac-NPs in dose and time dependent manner. For the total apoptotic cells was increase at the same concentration as time increasing. In addition, the late stage of apoptotic cells was also increased from 0.8 to 5.9% at the concentration of 5 μM and from 1.7 to 40.6% at the concentration of 10 μM when time was extended from 12 to 24 h. The results demonstrated that Smac-NPs could efficiently induce cancer cell apoptosis in the dose- and time-dependent manner.

Mechanism Involved in Stimulating Cell Apoptosis. Smac is an antagonist of XIAPs. Within the cells, SmacN7 can target XIAPs and then promote caspase pathways, finally reverse the antiapoptosis of cancer cells. In cancer cells, caspase pathway is inactive and an antiapoptotic protein Bcl-2 is overexpressed, contributing to the characteristic of antiapoptosis of cancer. Bax, a member of the Bcl-2 family, is an pro-apoptotic protein and play an important role in apoptosis regulation.[35] In the further research, we explored the mechanism involved in the stimulation of cancer cell apoptosis. MDA-MB-231 and H460 cells were treated with Smac-NPs at different concentration of 5, 10, and 15 μM for 24 h. And then protein level of pro-caspase-3 and Bcl-2 were detected by western-blot. As shown in Figure 5A, the expression of pro-caspase-3 was down-regulated as we increased the concentration of Smac-NPs in both MDA-MB-231 and H460, indicating that pro-caspase-3 might cleave into active-caspase-3. The expression of Bcl-2 in cancer cells was also decreased as a result of the exposure of MDA-MB-231 and H460 cells to Smac-NPs in a dose-independent manner. On the other hand, expression of Bax was up-regulated by Smac-NPs in both MDA-MB-231 and H460 cells. Regarding that Smac peptide could not directly interact with Bcl-2, we also studied the mechanism underlying the Bcl-2 loss. As NF-kB was identified as regulator of Bcl-2 and the inhibition of NF-kB could increase the Bax expression to induce apoptosis, we evaluated the expression of NF-kB-p65 subunit.[35,36] As shown in Figure S5 in the Supporting Information, NF-kB-p65 expression was suppressed by Smac-NPs, which might contribute to the down-regulation of Bcl-2 and up-regulation of Bax. Moreover, it seemed that pro-caspase-8 was not changed, which indicated that TNF-α signaling was not activated to induce apoptosis. Our results showed that Smac-NPs promoted cancer cells apoptosis through activating pro-caspase-3 cleavage, down-regulating Bcl-2 expression and up-regulation of Bax. Smac-NPs might induce cancer cell apoptosis in mitochondrial-dependent pathway. Schematic illustration of the mechanism is shown in Figure 5B.

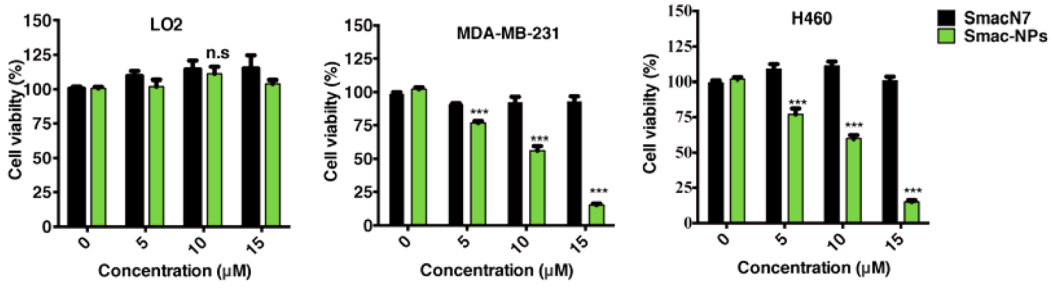

Figure 3. Cytotoxicity of SmacN7 and Smac-NPs on human normal cells LO2 and cancer cells MDA-MB-231 and H460. ***, $p < 0.001$ compared with the corresponding control value; n.s, no significance.

DOI: 10.1021/acsami.5b00329
ACS Appl. Mater. Interfaces 2015, 7, 8005−8012

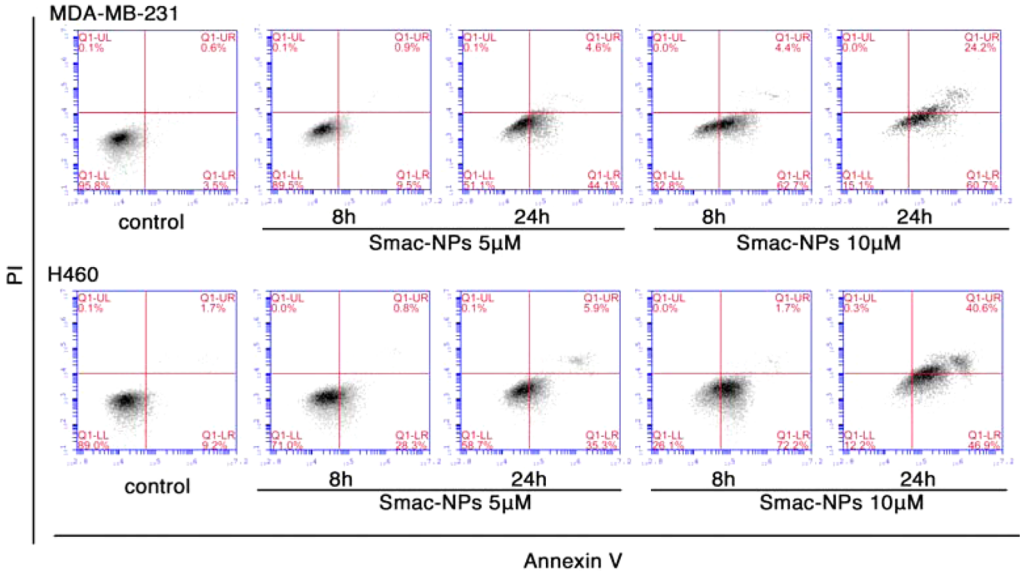

Figure 4. Cell apoptosis induced by Smac-NPs in MDA-MB-231 and H460 cells. MDA-MB-231 and H460 cells were exposed to Smac-NPs at the concentration of 5 and 10 μM for 8 and 24 h and the cell apoptosis was detect by flow cytometry. The first quadrant (Q1-LL) represented the live normal cells. Q1-LR represents the percentage of cells undergoing early apoptosis, whereas Q2-UR represents the percentage of cells at the late stage of apoptosis.

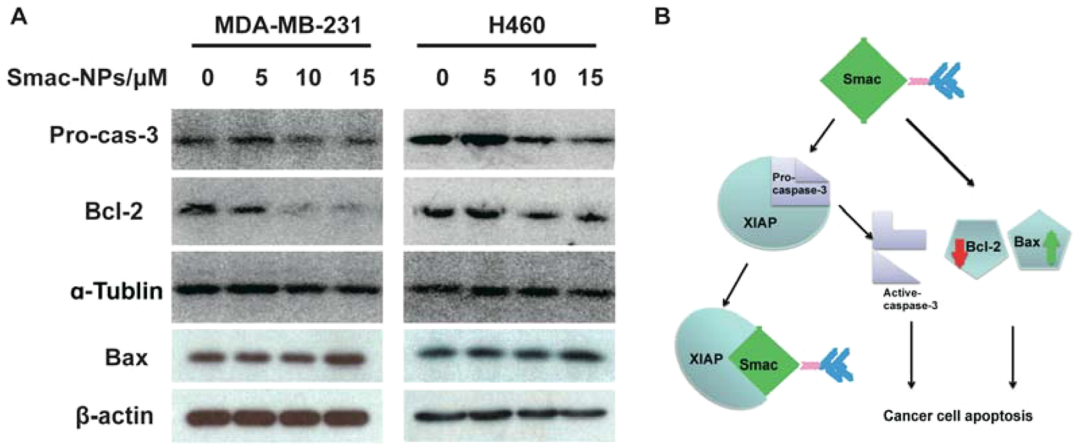

Figure 5. Expression of pro-caspase-3, Bcl-2, and Bax in MDA-MB-231 and H460 cells after treatment with Smac-NPs. Cells were treated with Smac-NPs at the concentration of 5, 10, and 15 μM for 48 h, and total protein was extracted and analyzed by western-blot assay. (A) Western-blot result for the expression of pro-caspase-3, Bcl-2, and Bax in MDA-MB-231 and H460 cells. (B) Schematic illustration of the mechanism involved in the Smac-NP-induced cancer cell apoptosis.

Cellular Uptake of DOX-Smac-NPs and Enhanced DOX Delivery Efficiency. Smac-conjugated polymer was designed not only as a pro-apoptotic compound but also as drug carrier when self-assembled into micelles. It is a targeted, double functioned drug delivery nanoparticle, which could be prospectively extended into multiple-function in further. DOX was loaded in Smac-NPs through oil-in-water emulsion method and the loading efficiency was up to 90%. Intercellular trafficking of DOX-loaded Smac-NPs (DOX-Smac-NPs) was determined by confocal laser scanning microscopy (CLSM) and DOX delivery efficiency was investigated by flow cytometry.

MDA-MB-231 and H460 cells were treated with free DOX and FAM-labeled DOX-Smac-NPs for 4 h and cellular uptake of DOX was detected and shown in Figure 6. We detected the localization of DOX in nuclear of MDA-MB-231 and H460 cells after incubation for 4 h. Our studies demonstrated that DOX was successfully encapsulated by Smac-NPs and cellular uptake of free DOX and DOX-Smac-NPs in MDA-MB-231 and H460 could be detected by CLSM.

Meanwhile, DOX delivery efficiency of DOX-Smac-NPs and free DOX were evaluated by flow cytometry. We detected cellular uptake of DOX after treatment with DOX-Smac-NPs and free DOX respectively at different time plots, 1, 2, 4, and 8 h. As shown in Figure 7, cellular uptake of DOX-Smac-NPs group was enhanced more significantly as time increased compared with the group of free DOX in both MDA-MB-231 cells (Figure 7A, B) and H460 cells (Figure 7C, D). Our result suggested that Smac-NPs could enhance the DOX delivery efficiency in cancer cells, which provided an approach to deliver the chemotherapeutics to cancer more powerful.

Cytotoxicity of DOX-Loaded Nanoparticles. To investigate the synergistic effect of DOX and Smac-NPs in vitro, we detected the cytotoxicity of free DOX, Smac-NPs and DOX-

DOI: 10.1021/acsami.5b00329
ACS Appl. Mater. Interfaces 2015, 7, 8005−8012

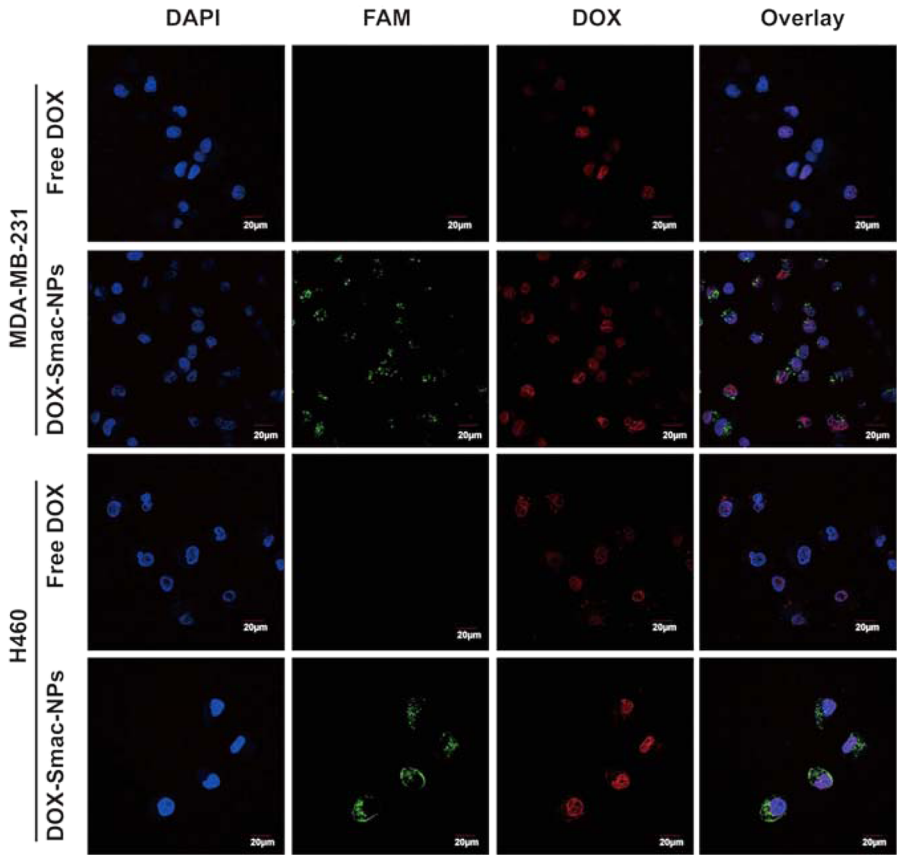

Figure 6. Confocal microscopy imaging of cellular uptake of free DOX and DOX-Smac-NPs in MDA-MB-231 and H460 cells after incubation for 4 h (1 μg/mL of DOX concentration). Smac-NPs and DOX-Smac-NPs were labeled with fluorescein amidite (FAM, green).

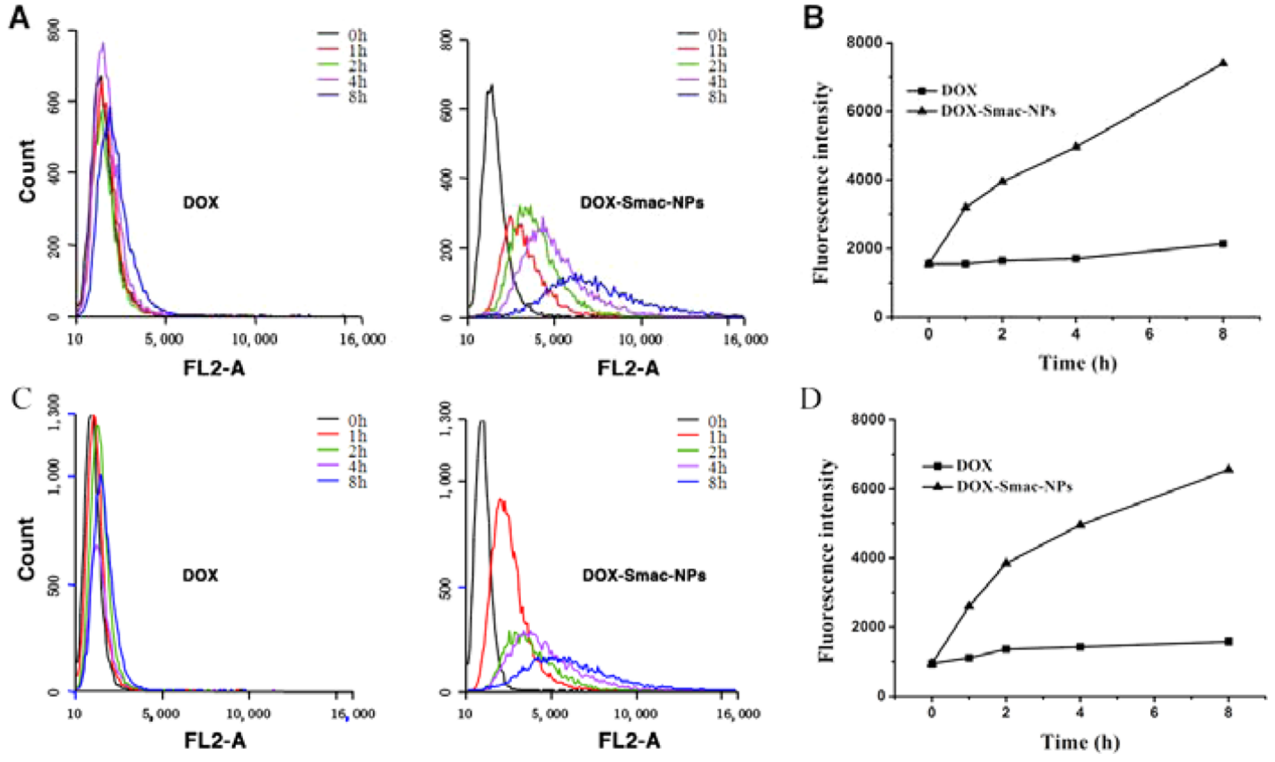

Figure 7. DOX delivery efficiency of DOX-Smac-NPs and free DOX in MDA-MB-231 and H460 cells. MDA-MB-231 and H460 cells were incubated with DOX-Smac-NPs and free DOX for 2 h and DOX delivery efficiency was determined by flow cytometry (0.01 μg/mL of DOX concentration). (A, B) MDA-MB-231, (C, D) H460.

DOI: 10.1021/acsami.5b00329
ACS Appl. Mater. Interfaces 2015, 7, 8005−8012

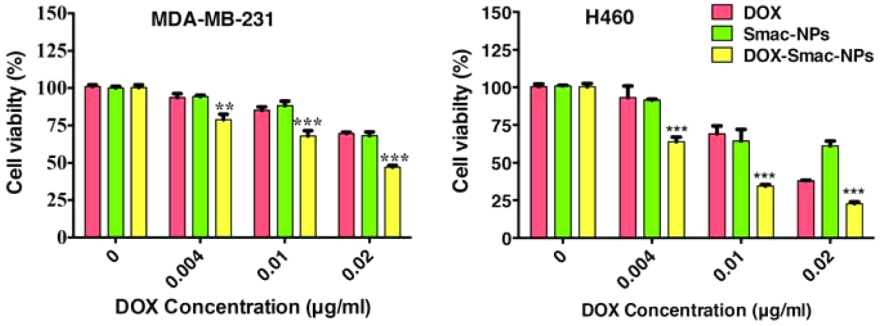

Figure 8. In vitro cytotoxicity of free DOX, Smac-NPs, and DOX-Smac-NPs on MDA-MB-231 and H460. The cells variety was examined by CCK-8 after 48 h of treatment. The concentration of Smac-NPs(μM): DOX(μg/mL) was 5:0.02, 2.5:0.01, and 0.1:0.004. **, $p < 0.01$, ***, $p < 0.001$ compared with the free DOX group and Smac-NPs group.

Smac-NPs on the two cancer cell lines by MTT assay as shown in Figure 8. The cell viability of both MDA-MB-231 and H460 was inhibited by free DOX, Smac-NPs, and DOX-Smac-NPs. For MDA-MB-231, as the concentration of DOX increased up to 0.02 μg/mL, cell viability was decreased nearly only 20%. However, the antiproliferation of DOX-Smac-NPs on MDA-MB-231 cells was enhanced significantly compared to that of free DOX and Smac-NPs at 0.004 μg/mL up to 0.02 μg/mL of DOX concentration, indicating the dose-dependent behavior. Meanwhile, DOX-Smac-NPs could significantly inhibit the cell viability of H460 compared with free DOX and Smac-NPs as well. The IC_{50} are shown in Table 1.

Table 1. IC_{50} of Free DOX and DOX-Smac-NPs in MDA-MB-231 and H460

cell line	group	IC_{50}(μg/mL) Mean ± SEM
MDA-MB-231	DOX	0.04 ± 0.004
	DOX-Smac-NPs	0.018 ± 0.001[b]
H460	DOX	0.023 ± 0.003
	DOX-Smac-NPs	0.009 ± 0.002[a]

[a] $p < 0.05$. [b] $p < 0.001$ compared with the free DOX group.

The IC50 of DOX-Smac-NPs was decreased over one time compared to that of free DOX. As we demonstrated above, Smac-NPs could inhibit cancer cell proliferation via inducing cancer cell apoptosis and could increase the cellular uptake of DOX, which might contribute to the enhanced antiproliferative effect of DOX-Smac-NPs. Smac-NPs may enhance DOX efficiency significantly on cancer cells by the combination therapy together. This highlights a new way to integrate the therapeutic peptide nanoparticles with the chemotherapeutics for a combination therapy of cancer.

CONCLUSION

A novel Smac-conjugated nanoparticle (Smac-NP) was designed with a SmacN7 peptide, cell penetration peptide and four hydrophobic tails. The Samc-NPs not only induced cell apoptosis through activation of caspase-3, down-regulation of the expression of Bcl-2 and up-regulation of Bax, but also encapsulated DOX chemotherapeutics efficiently. Such DOX-Smac-NPs could penetrate into tumor cells much easier, increasing the cellular uptake of DOX and further enhancing the pro-apoptotic role. Our work provided a new concept in designing multiple functional nanoparticles with targeting peptide groups, and paved a new insight into therapeutic peptide nanoparticles codelivering with drug for cancer combination therapy.

ASSOCIATED CONTENT

Supporting Information

HPLC analysis report of Smac-conjugated polymer, MS analysis of Smac-conjugated polymer, ^{1}H-NMR spectra of Smac-conjugated polymer, size stability of Smac-NPs, detection of expression level of NF-kB-p65 and pro-caspase-8 by western-blot. This material is available free of charge via the Internet at http://pubs.acs.org/.

AUTHOR INFORMATION

Corresponding Author

*E-mail: lt.cai@siat.ac.cn.

Notes

The authors declare no competing financial interest.

ACKNOWLEDGMENTS

The authors gratefully acknowledge support for the National Natural Science Foundation of China (Grants 81171446, 81371679, 21404115), Guangdong Innovation Team of Low-cost Healthcare, The Science and Technology Foundation of Guangdong (2012B090400043, 2012B090600036) and Shenzhen (JCYJ20130401170306862).

REFERENCES

(1) Wu, G.; Chai, J.; Suber, T. L.; Wu, J. W.; Du, C.; Wang, X.; Shi, Y. Structural basis of IAP recognition by Smac/DIABLO. *Nature* **2000**, *408*, 1008−12.

(2) Riedl, S. J.; Renatus, M.; Schwarzenbacher, R.; Zhou, Q.; Sun, C. H.; Fesik, S. W.; Liddington, R. C.; Salvesen, G. S. Structural basis for the inhibition of caspase-3 by XIAP. *Cell* **2001**, *104*, 791−800.

(3) Du, C. Y.; Fang, M.; Li, Y. C.; Li, L.; Wang, X. D. Smac, a mitochondrial protein that promotes cytochrome c-dependent caspase activation by eliminating IAP inhibition. *Cell* **2000**, *102*, 33−42.

(4) Arnt, C. R.; Chiorean, M. V.; Heldebrant, M. P.; Gores, G. J.; Kaufmann, S. H. Synthetic Smac/DIABLO peptides enhance the effects of chemotherapeutic agents by binding XIAP and cIAP1 in situ. *J. Biol. Chem.* **2002**, *277*, 44236−43.

(5) Chai, J. J.; Du, C. Y.; Wu, J. W.; Kyin, S.; Wang, X. D.; Shi, Y. G. Structural and biochemical basis of apoptotic activation by Smac/DIABLO. *Nature* **2000**, *406*, 855−862.

(6) Sun, H.; Nikolovska-Coleska, Z.; Yang, C. Y.; Xu, L.; Tomita, Y.; Krajewski, K.; Roller, P. P.; Wang, S. Structure-based design, synthesis, and evaluation of conformationally constrained mimetics of the second mitochondria-derived activator of caspase that target the X-linked inhibitor of apoptosis protein/caspase-9 interaction site. *J. Med. Chem.* **2004**, *47*, 4147−50.

DOI: 10.1021/acsami.5b00329
ACS Appl. Mater. Interfaces 2015, 7, 8005−8012

(7) Sun, H.; Stuckey, J. A.; Nikolovska-Coleska, Z.; Qin, D.; Meagher, J. L.; Qiu, S.; Lu, J.; Yang, C. Y.; Saito, N. G.; Wang, S. Structure-based design, synthesis, evaluation, and crystallographic studies of conformationally constrained Smac mimetics as inhibitors of the X-linked inhibitor of apoptosis protein (XIAP). *J. Med. Chem.* **2008**, *51*, 7169−80.
(8) Liu, Z.; Sun, C.; Olejniczak, E. T.; Meadows, R. P.; Betz, S. F.; Oost, T.; Herrmann, J.; Wu, J. C.; Fesik, S. W. Structural basis for binding of Smac/DIABLO to the XIAP BIR3 domain. *Nature* **2000**, *408*, 1004−8.
(9) Yang, L.; Mashima, T.; Sato, S.; Mochizuki, M.; Sakamoto, H.; Yamori, T.; Oh-Hara, T.; Tsuruo, T. Predominant suppression of apoptosome by inhibitor of apoptosis protein in non-small cell lung cancer H460 cells: therapeutic effect of a novel polyarginine-conjugated Smac peptide. *Cancer Res.* **2003**, *63*, 831−7.
(10) Sun, H.; Nikolovska-Coleska, Z.; Yang, C. Y.; Qian, D.; Lu, J.; Qiu, S.; Bai, L.; Peng, Y.; Cai, Q.; Wang, S. Design of small-molecule peptidic and nonpeptidic Smac mimetics. *Acc. Chem. Res.* **2008**, *41*, 1264−77.
(11) Bai, L.; Xu, S.; Chen, W.; Li, Z.; Wang, X.; Tang, H.; Lin, Y. Blocking NF-kappaB and Akt by Hsp90 inhibition sensitizes Smac mimetic compound 3-induced extrinsic apoptosis pathway and results in synergistic cancer cell death. *Apoptosis* **2011**, *16*, 45−54.
(12) Chen, K. F.; Lin, J. P.; Shiau, C. W.; Tai, W. T.; Liu, C. Y.; Yu, H. C.; Chen, P. J.; Cheng, A. L. Inhibition of Bcl-2 improves effect of LCL161, a SMAC mimetic, in hepatocellular carcinoma cells. *Biochem. Pharmacol.* **2012**, *84*, 268−77.
(13) Nikolovska-Coleska, Z.; Meagher, J. L.; Jiang, S.; Yang, C. Y.; Qiu, S.; Roller, P. P.; Stuckey, J. A.; Wang, S. Interaction of a cyclic, bivalent smac mimetic with the x-linked inhibitor of apoptosis protein. *Biochemistry* **2008**, *47*, 9811−24.
(14) Lu, J.; Bai, L.; Sun, H.; Nikolovska-Coleska, Z.; McEachern, D.; Qiu, S.; Miller, R. S.; Yi, H.; Shangary, S.; Sun, Y.; Meagher, J. L.; Stuckey, J. A.; Wang, S. SM-164: a novel, bivalent Smac mimetic that induces apoptosis and tumor regression by concurrent removal of the blockade of cIAP-1/2 and XIAP. *Cancer Res.* **2008**, *68*, 9384−93.
(15) Lu, J.; McEachern, D.; Sun, H.; Bai, L.; Peng, Y.; Qiu, S.; Miller, R.; Liao, J.; Yi, H.; Liu, M.; Bellail, A.; Hao, C.; Sun, S. Y.; Ting, A. T.; Wang, S. Therapeutic potential and molecular mechanism of a novel, potent, nonpeptide, Smac mimetic SM-164 in combination with TRAIL for cancer treatment. *Mol. Cancer Ther.* **2011**, *10*, 902−14.
(16) Yang, D.; Zhao, Y.; Li, A. Y.; Wang, S.; Wang, G.; Sun, Y. Smac-mimetic compound SM-164 induces radiosensitization in breast cancer cells through activation of caspases and induction of apoptosis. *Breast Cancer Res. Treat.* **2012**, *133*, 189−99.
(17) Sun, W.; Nikolovska-Coleska, Z.; Qin, D.; Sun, H.; Yang, C. Y.; Bai, L.; Qiu, S.; Wang, Y.; Ma, D.; Wang, S. Design, synthesis, and evaluation of potent, nonpeptidic mimetics of second mitochondria-derived activator of caspases. *J. Med. Chem.* **2009**, *52*, 593−6.
(18) Sun, H.; Nikolovska-Coleska, Z.; Yang, C. Y.; Xu, L.; Liu, M.; Tomita, Y.; Pan, H.; Yoshioka, Y.; Krajewski, K.; Roller, P. P.; Wang, S. Structure-based design of potent, conformationally constrained Smac mimetics. *J. Am. Chem. Soc.* **2004**, *126*, 16686−7.
(19) Dineen, S. P.; Roland, C. L.; Greer, R.; Carbon, J. G.; Toombs, J. E.; Gupta, P.; Bardeesy, N.; Sun, H. Z.; Williams, N.; Minna, J. D.; Brekken, R. A. Smac Mimetic Increases Chemotherapy Response and Improves Survival in Mice with Pancreatic Cancer. *Cancer Res.* **2010**, *70*, 2852−2861.
(20) Acharya, S.; Dilnawaz, F.; Sahoo, S. K. Targeted epidermal growth factor receptor nanoparticle bioconjugates for breast cancer therapy. *Biomaterials* **2009**, *30*, 5737−50.
(21) Liu, P.; Li, Z.; Zhu, M.; Sun, Y.; Li, Y.; Wang, H.; Duan, Y. Preparation of EGFR monoclonal antibody conjugated nanoparticles and targeting to hepatocellular carcinoma. *J. Mater. Sci. Mater. Med.* **2010**, *21*, 551−6.
(22) Liu, Y.; Li, K.; Pan, J.; Liu, B.; Feng, S. S. Folic acid conjugated nanoparticles of mixed lipid monolayer shell and biodegradable polymer core for targeted delivery of Docetaxel. *Biomaterials* **2010**, *31*, 330−8.
(23) Gong, P.; Shi, B.; Zheng, M.; Wang, B.; Zhang, P.; Hu, D.; Gao, D.; Sheng, Z.; Zheng, C.; Ma, Y.; Cai, L. PEI protected aptamer molecular probes for contrast-enhanced in vivo cancer imaging. *Biomaterials* **2012**, *33*, 7810−7.
(24) Zheng, C.; Zheng, M.; Gong, P.; Jia, D.; Zhang, P.; Shi, B.; Sheng, Z.; Ma, Y.; Cai, L. Indocyanine green-loaded biodegradable tumor targeting nanoprobes for in vitro and in vivo imaging. *Biomaterials* **2012**, *33*, 5603−9.
(25) Liu, P.; Shi, B. H.; Yue, C. X.; Gao, G. H.; Li, P.; Yi, H. Q.; Li, M. X.; Wang, B.; Ma, Y. F.; Cai, L. T. Dextran-based redox-responsive doxorubicin prodrug micelles for overcoming multidrug resistance. *Polym. Chem.* **2013**, *4*, 5793−5799.
(26) Farokhzad, O. C.; Langer, R. Impact of nanotechnology on drug delivery. *ACS Nano* **2009**, *3*, 16−20.
(27) Deng, J. Z.; Gao, N. N.; Wang, Y. A.; Yi, H. Q.; Fang, S. T.; Ma, Y. F.; Cai, L. T. Self-Assembled Cationic Micelles Based on PEG-PLL-PLLeu Hybrid Polypeptides as Highly Effective Gene Vectors. *Biomacromolecules* **2012**, *13*, 3795−3804.
(28) Chen, J. X.; Wang, H. Y.; Li, C.; Han, K.; Zhang, X. Z.; Zhuo, R. X. Construction of surfactant-like tetra-tail amphiphilic peptide with RGD ligand for encapsulation of porphyrin for photodynamic therapy. *Biomaterials* **2011**, *32*, 1678−84.
(29) Zheng, C.; Zheng, M.; Gong, P.; Deng, J.; Yi, H.; Zhang, P.; Zhang, Y.; Liu, P.; Ma, Y.; Cai, L. Polypeptide cationic micelles mediated co-delivery of docetaxel and siRNA for synergistic tumor therapy. *Biomaterials* **2013**, *34*, 3431−8.
(30) Zheng, M.; Yue, C.; Ma, Y.; Gong, P.; Zhao, P.; Zheng, C.; Sheng, Z.; Zhang, P.; Wang, Z.; Cai, L. Single-step assembly of DOX/ICG loaded lipid–polymer nanoparticles for highly effective chemo-photothermal combination therapy. *ACS Nano* **2013**, *7*, 2056−67.
(31) Meng, H.; Liong, M.; Xia, T.; Li, Z.; Ji, Z.; Zink, J. I.; Nel, A. E. Engineered design of mesoporous silica nanoparticles to deliver doxorubicin and P-glycoprotein siRNA to overcome drug resistance in a cancer cell line. *ACS Nano* **2010**, *4*, 4539−50.
(32) Bai, F.; Wang, C.; Lu, Q.; Zhao, M.; Ban, F. Q.; Yu, D. H.; Guan, Y. Y.; Luan, X.; Liu, Y. R.; Chen, H. Z.; Fang, C. Nanoparticle-mediated drug delivery to tumor neovasculature to combat P-gp expressing multidrug resistant cancer. *Biomaterials* **2013**, *34*, 6163−74.
(33) Liu, P.; Yue, C. X.; Shi, B. H.; Gao, G. H.; Li, M. X.; Wang, B.; Ma, Y. F.; Cai, L. T. Dextran based sensitive theranostic nanoparticles for near-infrared imaging and photothermal therapy in vitro. *Chem. Commun.* **2013**, *49*, 6143−6145.
(34) Qin, S. D.; Yang, C. C.; Li, S.; Xu, C. W.; Zhao, Y.; Ren, H. Smac: Its role in apoptosis induction and use in lung cancer diagnosis and treatment. *Cancer Lett.* **2012**, *318*, 9−13.
(35) Catz, S. D.; Johnson, J. L. Transcriptional regulation of bcl-2 by nuclear factor kappa B and its significance in prostate cancer. *Oncogene* **2001**, *20*, 7342−51.
(36) Bentires-Alj, M.; Dejardin, E.; Viatour, P.; Van Lint, C.; Froesch, B.; Reed, J. C.; Merville, M. P.; Bours, V. Inhibition of the NF-kappa B transcription factor increases Bax expression in cancer cell lines. *Oncogene* **2001**, *20*, 2805−13.

DOI: 10.1021/acsami.5b00329
ACS Appl. Mater. Interfaces 2015, 7, 8005−8012